Rainfall-runoff modelling using river stage time series in the absence of reliable discharge information: a case study in the semi-arid Mara River Basin

Petra Hulsman[1], Thom A. Bogaard[1], Hubert H.G. Savenije[1]

5   [1]Water Resources Section, Faculty of Civil Engineering and Geosciences, Delft University of Technology, Stevinweg 1, 2628 CN Delft, the Netherlands

Correspondence to: Petra Hulsman (p.hulsman@tudelft.nl)

Abstract. Hydrological models play an important role in Water Resources Management. These models generally rely on discharge data for calibration. Discharge time series are normally derived from observed water

10   levels by using a rating curve. However, this method suffers from many uncertainties due to insufficient observations, inadequate rating curve fitting procedures, rating curve extrapolation, and temporal changes in the river geometry. Unfortunately, this problem is prominent in many African river basins. In this study, an alternative calibration method is presented using water level time series instead of discharge, applied to a semi-distributed rainfall-runoff model for the semi-arid and poorly gauged Mara River Basin in Kenya. The modelled

15   discharges were converted into water levels using the Strickler-Manning formula. This method produces an additional model output: a "geometric rating curve equation" which relates the modelled discharge to the observed water level using the Strickler-Manning formula and a calibrated slope-roughness parameter. This procedure resulted in good and consistent model results during calibration and validation. The hydrological model was able to reproduce the water levels for the entire basin as well as for the Nyangores sub-catchment in

20   the north. The newly derived geometric rating curves were subsequently compared to the existing rating curves. At the catchment outlet of the Mara, these differed significantly, most likely due to uncertainties in the recorded discharge time series. However, at the 'Nyangores' sub-catchment, the geometric and recorded discharge were almost identical. In conclusion, the results obtained for the Mara river basin illustrate that with the proposed calibration method the water level time series can be simulated well, and that also the discharge-water level

25   relation can be derived, even in catchments with uncertain or lacking rating curve information.

1 Introduction to rating curve uncertainties

Hydrological models play an important role in Water Resources Management. In hydrological modelling, discharge time series are of crucial importance. For example, discharge is used when estimating flood peaks (Di Baldassarre et al., 2012;Kuczera, 1996), calibrating models (Domeneghetti et al., 2012;McMillan et al., 2010) or determining the model structure (McMillan and Westerberg, 2015;Bulygina and Gupta, 2011). Discharge is commonly measured indirectly through interpolation of velocity measurements over the cross-section (WMO, 2008;Di Baldassarre and Montanari, 2009). However, to obtain frequent or continues discharge data, this method is time consuming and cost-inefficient. Moreover, in African river catchments, the quantity and quality of the available discharge measurements is unfortunately often inadequate for reliable calibration of hydrological models (Shahin, 2002;Hrachowitz et al., 2013).

There are several sources of uncertainty in discharge data when using rating curves that cannot be neglected. First, measurement errors in the individual discharge measurements affect the estimated continuous discharge data, for example in the velocity-area method uncertainties in the cross-section and velocity can arise due to poor sampling (Pelletier, 1988;Sikorska et al., 2013). Second, these measurements are usually done during normal flows, however during floods the rating curve needs to be extrapolated. Therefore, the uncertainty increases for discharges under extreme conditions (Di Baldassarre and Claps, 2011;Domeneghetti et al., 2012). Thirdly, the fitting procedure does not always account well for irregularities in the profile, particularly when banks are overtopped. Finally, the river is a dynamic, non-stationary system which influences the rating curve, for example changes in the cross-section due to sedimentation or erosion, backwater effects or hysteresis (Petersen-Øverleir, 2006). The lack of incorporating such temporal changes in the rating curve increases the uncertainty in discharge data (Guerrero et al., 2012;Jalbert et al., 2011;Morlot et al., 2014). As a result, the rating curve should be regularly updated to take such changes into account. The timing of adjusting the rating curve relative to the changes in the river affects the number of rating curves and the uncertainty (Tomkins, 2014). Previous studies focused on assessing the uncertainty of rating curves (Di Baldassarre and Montanari, 2009;Clarke, 1999) and their effect on model predictions (Karamuz et al., 2016;Sellami et al., 2013;Thyer et al., 2011).

In the absence of reliable rating curves, remotely sensed river characteristics related to the discharge such as river width and water level can provide valuable information on the flow dynamics for model calibration and validation. For instance, previous studies derived the discharge from remotely sensed river width (Revilla-Romero et al., 2015;Yan et al., 2015;Sun et al., 2015) or river water levels measured with radar altimetry (Pereira-Cardenal et al., 2011;Michailovsky et al., 2012;Ričko et al., 2012;Schwatke et al., 2015;Tourian et al., 2017;Sun et al., 2012). In previous studies, hydrological models were calibrated on river width or surface water extent (Sun et al., 2015;Revilla-Romero et al., 2015). Also radar altimetry observations of river water levels have been used to calibrate or validate hydrological models by using empirical equations transforming discharge to water level without using cross-section information (Sun et al., 2012;Getirana, 2010), for instance conceptual hydrological models (Sun et al., 2012;Pereira-Cardenal et al., 2011) or process-based models (Getirana, 2010;Paiva et al., 2013).

Besides remotely sensed river characteristics, also locally measured river water level time series are valuable for model calibration and validation (van Meerveld et al., 2017). In general, water levels time series are more reliable than discharge data or remotely sensed river characteristics as these are direct measurements and not

processed data. In previous studies, hydrological models have been calibrated on river water level time series using the Spearman rank correlation coefficient (Jian et al., 2017;Seibert and Vis, 2016) or by including an inverse rating curve with three new calibration parameters to convert the modelled discharge to water level (Jian et al., 2017). When using the Spearman rank correlation function, the focus is on correlating the ranks instead of

70   the magnitudes, which as a result introduces biases in the model results. Alternatively, rainfall-runoff models can be calibrated on water level time series combined with a hydraulic equation introducing only one new calibration parameter. Also data-driven models have been calibrated successfully on water level time series, for example artificial neural network or fuzzy logic approaches were applied (Liu and Chung, 2014;Panda et al., 2010;Alvisi et al., 2006).

75   The goal of this study is to illustrate the potential of water level time series for hydrological model calibration by incorporating a hydraulic equation describing the rating curve within the model. This calibration method is applied to the semi-arid and poorly gauged Mara River Basin in Kenya. For three gauging stations within this basin, the quality of the recorded rating curves have been analysed and compared to the model results. For this purpose, a semi-distributed rainfall-runoff model has been developed on a daily timescale applying the FLEX-

80   Topo modelling concept (Savenije, 2010).

2 Site description of the Mara River Basin and data availability

The Mara River originates in Kenya in the Mau Escarpment and flows through the Masai Mara National Reserve in Kenya into Lake Victoria in Tanzania. The main tributaries are the Nyangores and Amala Rivers in the upper reach and the Lemek, Talak and Sand in the middle reach (Figure 1). The first two tributaries are perennial while the remaining tributaries are ephemeral, which generally dry out during dry periods. In total, the river is 395 km long (Dessu et al., 2014) and its catchment covers an area of about 11,500 km^2 (McClain et al., 2013) of which 65% is located in Kenya (Mati et al., 2008).

Within the Mara River Basin, there are two wet seasons linked to the annual oscillations of the ITCZ (Inter-tropical Convergence Zone). The first wet season is from March to May and the second from October to December (McClain et al., 2013). The precipitation varies spatially over the catchment following the local topography. The largest annual rainfall can be found in the upstream area of the catchment: between 1000 and 1750 mm/yr. In the middle and downstream areas, the annual rainfall is between 900 and 1000 mm/yr and between 300 and 850 mm/yr, respectively (Dessu et al., 2014).

The elevation of the river basin varies between 3000 m above sea level at the Mau Escarpment, 1480 m at the border to Tanzania and 1130 m at Lake Victoria (McClain et al., 2013). In the Mara River Basin, the main land cover types are agriculture, grass, shrubs and forests. The main forest in the catchment is the Mau Forest, which is located in the north. Croplands are mainly found in the north and in the south, whereas the middle part is dominated by grasslands.

2.1 Data availability

2.1.1 In situ monitoring data

In the Mara River Basin, long term daily water level and discharge time series are available for 44-60 years between 1955 and 2015 at the downstream station near Mines and in the two main tributaries: the Nyangores and Amala. In addition, precipitation and air temperature is measured at 27 and 7 stations, respectively (Figure 1 and Table 1). However, the temporal coverage of these data is poor as there are many gaps.

There are many uncertainties in the discharge and precipitation data in the Mara River Basin. Discharge data analyses indicated that the time series were unreliable due to various inconsistencies in the data, especially at Mines and Amala. At Mines, a high scatter in the discharge-water level graph was observed (Figure 2); also back-calculated cross-section average flow velocities were below 1 m/s (Figure S1) whereas in 2012 the measured velocity was 2.13 m/s and discharge 529.3 m^3/s (GLOWS-FIU, 2012). At Amala, the rating curves were adjusted multiple times affecting mostly the low flows. Only the rating curve at Nyangores was stable and consistent with field measurements. The precipitation data analysis showed a high spatial variability between the limited number of rainfall stations available. More information can be found in the supplement "S1 Data quality".

During field trips, point discharge measurements were done in September/October 2014 at Emarti Bridge, Serena Pump House and New Mara Bridge, see Table 2 and Figure 3. At each location, the discharge was derived using an Acoustic Doppler Profiler (Sontek RiverSurveyor M9) mounted on a portable raft which is also equipped with a Power Communications Module and a DGPS antenna (Rey et al., 2015).
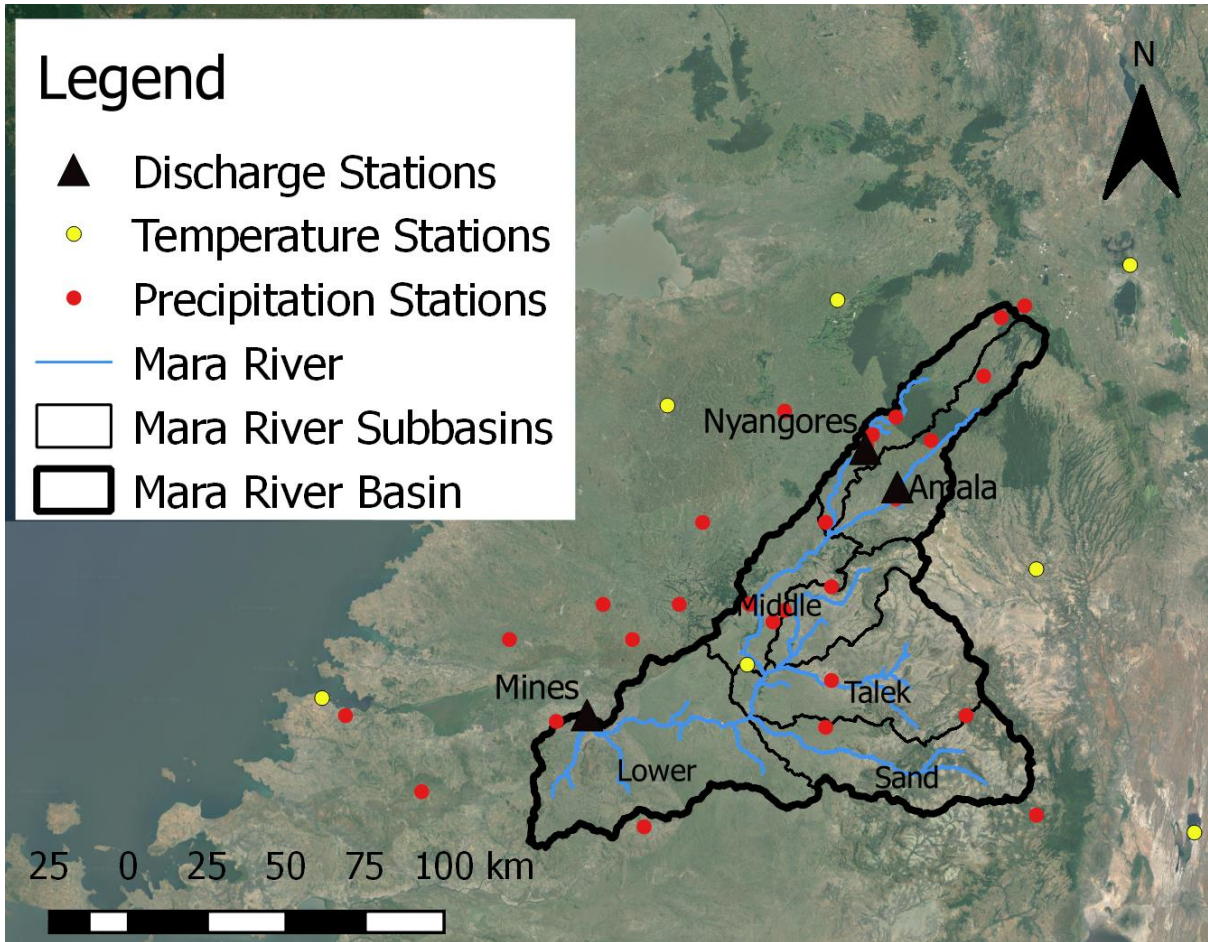
Figure 1: Map of the Mara River Basin and the hydro-meteorological stations for which data is available
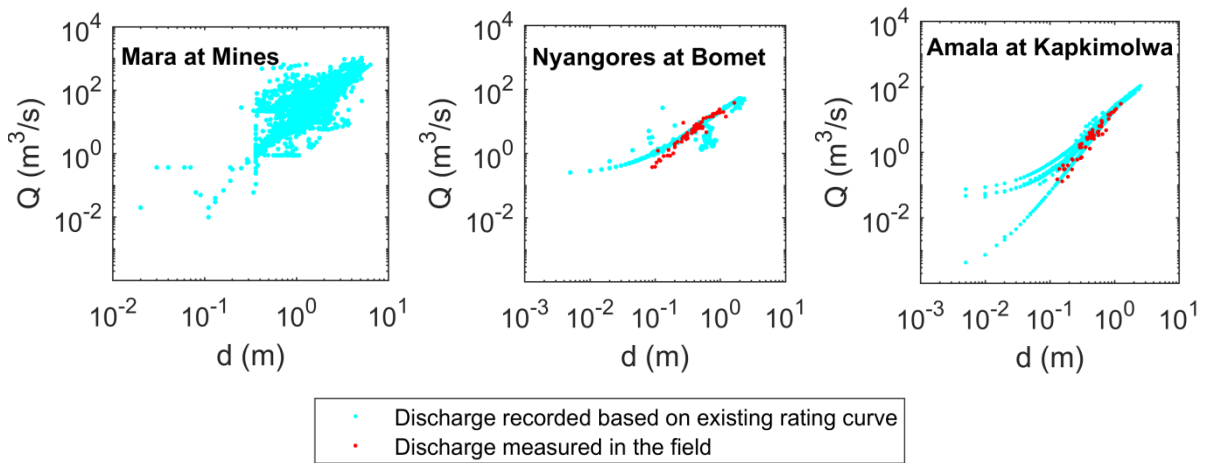
Figure 2: Discharge - water depth graphs for the three main river gauging stations in the Mara River Basin: Mara at Mines, Nyangores at Bomet and Amala at Kapkimolwa. 1) Recorded discharge and water level time series between 1960 and 2010 (light blue), 2) discharge field measurements from the Nile Decision Support Tool (NDST) for the time period 1963 - 1989 (Nyangores) and 1965 - 1992 (Amala), no data was available for Mines (red)

Table 1: Hydro-meteorological data availability in the Mara River Basin. The temporal coverage for water level and discharge can be different due to poor administration.

	Precipitation	Temperature	Water level, discharge		
Number of stations	28	7	3		
Station ID	-	-	1LA03	1LB02	5H2
Station location	-	-	Nyangores at Bomet	Amala at Kapkimolwa	Mara at Mines
Time range	1959 -2011	1957 - 2014	1963-2009	1955-2015	1969-2013
Duration [years]	0 - 43	3 - 57	46	60	44
Coverage	8 - 100%	30 -100%	Discharge: 85% Water level: 85%	Discharge: 72% Water level: 70%	Discharge: 53% Water level: 61%

135 **Table 2: Discharge measured in the field using an Acoustic Doppler Profiler (Sontek RiverSurveyor M9) mounted on a portable raft which is also equipped with a Power Communications Module and a DGPS (Rey et al., 2015)**

Station name	Date	Mean discharge	Standard deviation
Emarti Bridge	13 Sep 2014	19.2 m^3/s	0.7 m^3/s
	4 Oct 2014	13.4 m^3/s	0.6 m^3/s
Serena Pump House	9 Oct 2014	16.6 m^3/s	0.4 m^3/s
New Mara Bridge	19 Sep 2014	19.6 m^3/s	0.6 m^3/s
	6 Oct 2014	21.9 m^3/s	0.4 m^3/s
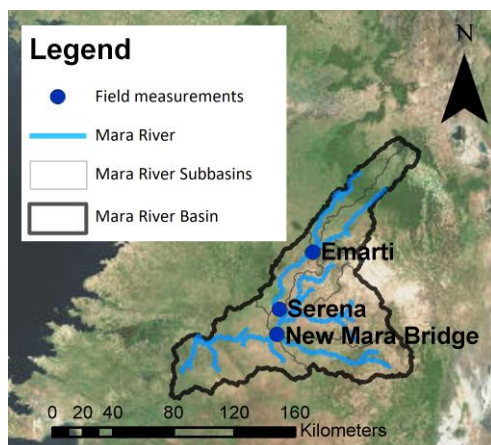
Figure 3: Map of discharge measurement locations during field trips in September/October 2014

140 **2.1.2 Remotely sensed data**

Besides ground observations, also remotely sensed data were used for setting up the rainfall-runoff model. Catchment classification was based on topography and land cover. For the topography, a digital elevation map (SRTM) with a resolution of 90 m and vertical accuracy of 16 m was used (U.S. Geological Survey, 2014). The land cover was based on Africover, a land cover database based on ground truth and satellite images (FAO,

145 1998). For the climate, remotely sensed precipitation was used from FEWSNET on a daily timescale from 2001 to 2010 and monthly actual evaporation from USGS from 2001 to 2013. Moreover, NDVI maps derived from Landsat images were used to define parameter constraints.

3 Hydrological model setup for the Mara River Basin

3.1 Catchment classification based on landscape and land use

150   For this study, the modelling concept of FLEX-Topo has been used (Savenije, 2010). It is a semi-distributed rainfall-runoff modelling framework that distinguishes hydrological response units (HRUs) based on landscape features. The landscape classes were identified based on the topographical indices HAND (Height Above Nearest Drain) and slope using a digital elevation map. Hillslopes are defined by a strong slope and high HAND, wetlands by a low HAND, and terraces by a high HAND and mild slope. The threshold for the slope

155   (21.9%) was based on a sensitivity analyses within the Mara Basin which revealed that the area of hillslopes changed asymptotically with the threshold. Therefore, the slope threshold was chosen at the point where changes in the sloped area become insignificant. As the wetland area was insignificant based on field observations, the HAND threshold was set to zero. In the Mara River Basin, there are mainly terraces and hillslopes.

160   To further delimit these two main landscape units, the land cover is taken into account as well. In the upper sub-catchments, there are mainly croplands and forests, whereas further south the land use is dominated by grasslands. In the lower sub-catchment, there are mostly croplands and grasslands. This resulted in four HRUs within the sub-basin of the Mara River Basin: forested hillslopes, shrubs on hillslopes, agriculture and grassland (Figure 4, Figure 5 and Table 3).

165

Table 3: Classification results: area percentage of each hydrological response unit per sub-catchment in the Mara River Basin

Sub-catchment	Agriculture	Shrubs on hillslopes	Grassland	Forested hillslopes
Amala	67%	0%	0%	33%
Nyangores	61%	0%	0%	39%
Middle	19%	16%	65%	0%
Lemek	10%	39%	51%	0%
Talek	0%	21%	79%	0%
Sand	0%	42%	58%	0%
Lower	26%	23%	52%	0%
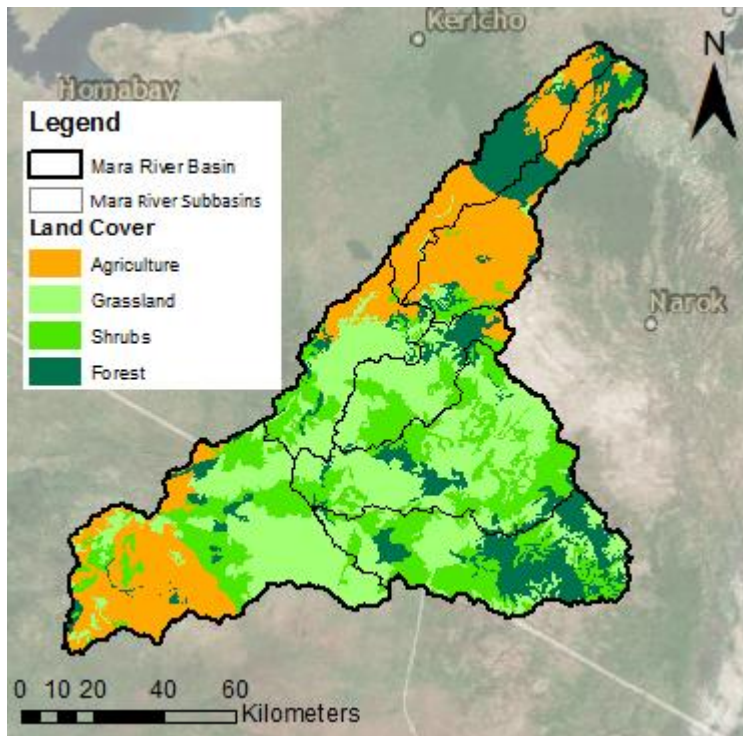
170

Figure 4: Classification of the Mara River Basin into four hydrological response units for each sub-catchment based on land use and landscape

3.2 Hydrological model structure

175 Each HRU is represented by a lumped conceptual model; the model structure is based on the dominant flow processes observed during field trips or deducted from interviews with local people. For example, in forests and shrub lands, Shallow Subsurface Flow (SSF) was seen to be the dominating flow mechanism: Rainwater infiltrates into the soil and flows through preferential flow paths to the river. In contrast, grassland and cropland generate overland flow. The observed soil compaction, due to cattle trampling and ploughing, reduces the
180 preferential infiltration capacity resulting in overland flow during heavy rainfall. Consequently, there Hortonian Overland Flow (HOF) occurs at high rainfall intensities excessing the maximum infiltration capacity. The perception of the dominant flow mechanisms (Figure 5) was then used to develop the model structure (Figure 6). This approach of translating a perceptual model into a model concept (Beven, 2012) was applied successfully in previous FLEX-Topo applications (Gao et al., 2014a;Gharari et al., 2014).

185 The model structure contains multiple storage components schematised as reservoirs (Figure 6). For each reservoir, the inflow, outflow and storage are defined by water balance equations, see Table 4. Process equations determine the fluxes between these reservoirs as a function of input drivers and their storage. HRUs function in parallel and independently from each other. However, they are connected through the groundwater system and the drainage network. To find the total runoff at the sub-catchment outlet $Q_{m,sub}$, the outflow $Q_{m,i}$ of each HRU is
190 multiplied by its relative area and then added up together with the groundwater discharge Q_s. The relative area is the area of a specific HRU divided by the entire sub-catchment area. Subsequently, the modelled discharge at the catchment outlet is obtained by using a simple river routing technique where a delay from sub-catchment outlet to catchment outlet was added assuming an average river flow velocity of 0.5 m/s. In the Sand sub-

catchment, it is schematised that runoff can percolate to the groundwater from the river bed and that moisture

195   can evaporate from the groundwater through deep rooting or riparian vegetation.

Table 4: Equations applied in the hydrological model. The formulas for the unsaturated zone are written for the hydrological response units: *Forested hillslopes* and *Shrubs on hillslopes*; for grass and agriculture, the inflow P_e changes to Q_F. The modelling time step is Δt = 1 day. Note that at a time daily step, the transfer of interception storage between consecutive days is assumed to be negligible.

Reservoir system	Water balance equation	Process functions
Interception	$\frac{\Delta S_i}{\Delta t} = P - P_e - E_i \approx 0$	$E_i = \min(E_p, \min(P, I_{max}))$
Surface	$\frac{\Delta S_o}{\Delta t} = P_e - Q_F - Q_{HOF} - E_o$	$Q_F = \min(\frac{S_o}{\Delta t}, F_{max})$
		$Q_{HOF} = \max\frac{(0, S_o - S_{max})}{\Delta t}$
		$E_o = \max(0, \min(E_p - E_i, \frac{S_o}{\Delta t}))$
Unsaturated zone	$\frac{\Delta S_u}{\Delta t} = (1 - C) * P_e - E$	$C = 1 - \left(1 - \frac{S_u}{S_{u,max}}\right)^\beta$
		$E = \min((E_p - E_i), \min\left(\frac{S_u}{\Delta t}, (E_p - E_i) * \frac{S_u}{S_{u,max}} * \frac{1}{C_e}\right))$
Groundwater recharge		$R_s = W * C * P_e$
Fast runoff	$\frac{\Delta S_f}{\Delta t} = R_{fl} - Q_f$	$R_{fl} = T_{lag}(C * P_e - R_s) \rightarrow$ in a linear delay function T_{lag}
		$Q_f = \frac{S_f}{K_f}$
Groundwater	$\frac{\Delta S_s}{\Delta t} = R_{s,tot} - Q_s - E_s + Q_{inf}$	$R_{s,tot} = \sum_{i=1}^{i=4} R_{s;HRU_i}$
		$Q_s = \frac{S_s}{K_s}$
		$E_s = 0$ and $Q_{inf} = 0$ for all sub $-$ basins except Sand
		$Q_{inf} = \min\left(\frac{S_{s,max} - S_s}{\Delta t}, Q_f\right)$ for Sand sub $-$ basin
		$E_s = \max\left(0, \min\left(E_p - E_i - E_o - E, \frac{S_s}{\Delta t}\right)\right)$ for Sand sub $-$ basin
Total runoff		$Q_m = Q_s + \sum_{i=1}^{i=4} Q_{f;HRU_i}$

| Hillslope | Hillslope | Terrace | | Terrace | Hillslope |

| Forest | Shrubs | Grassland | | Agriculture | Agriculture |

| SSF | SSF | HOF | | HOF | HOF |
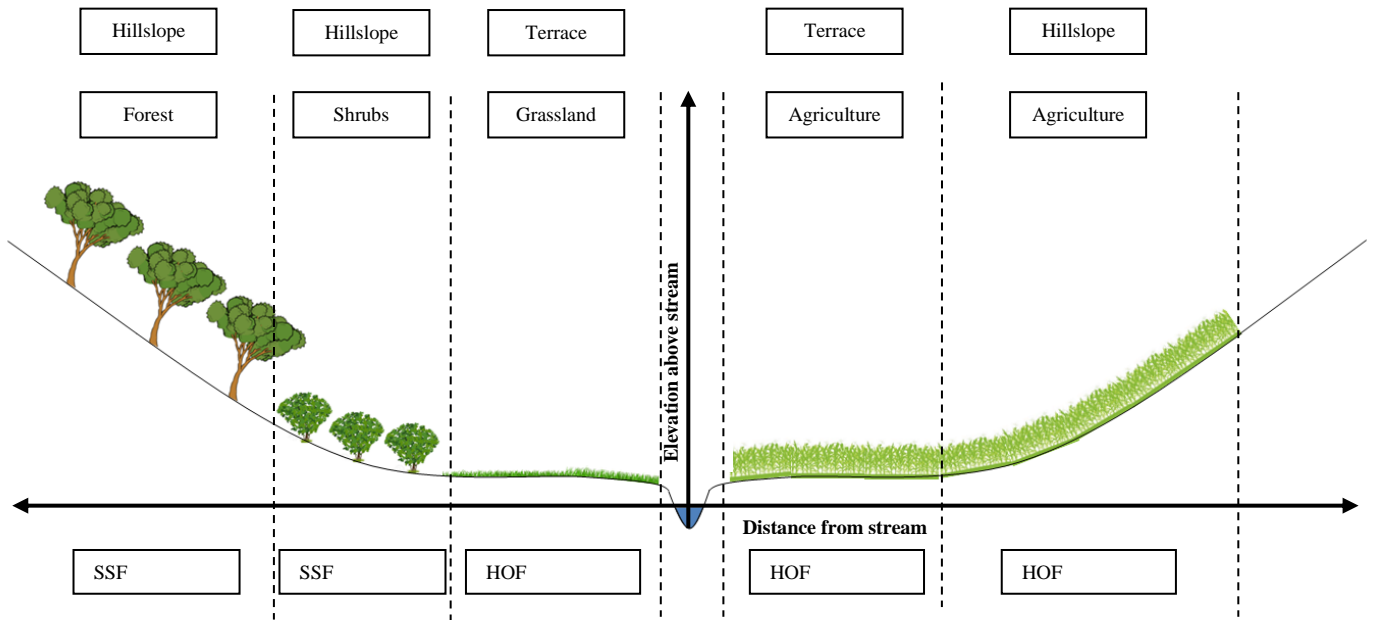
Figure 5: Schematization of the landscape and land use based classification
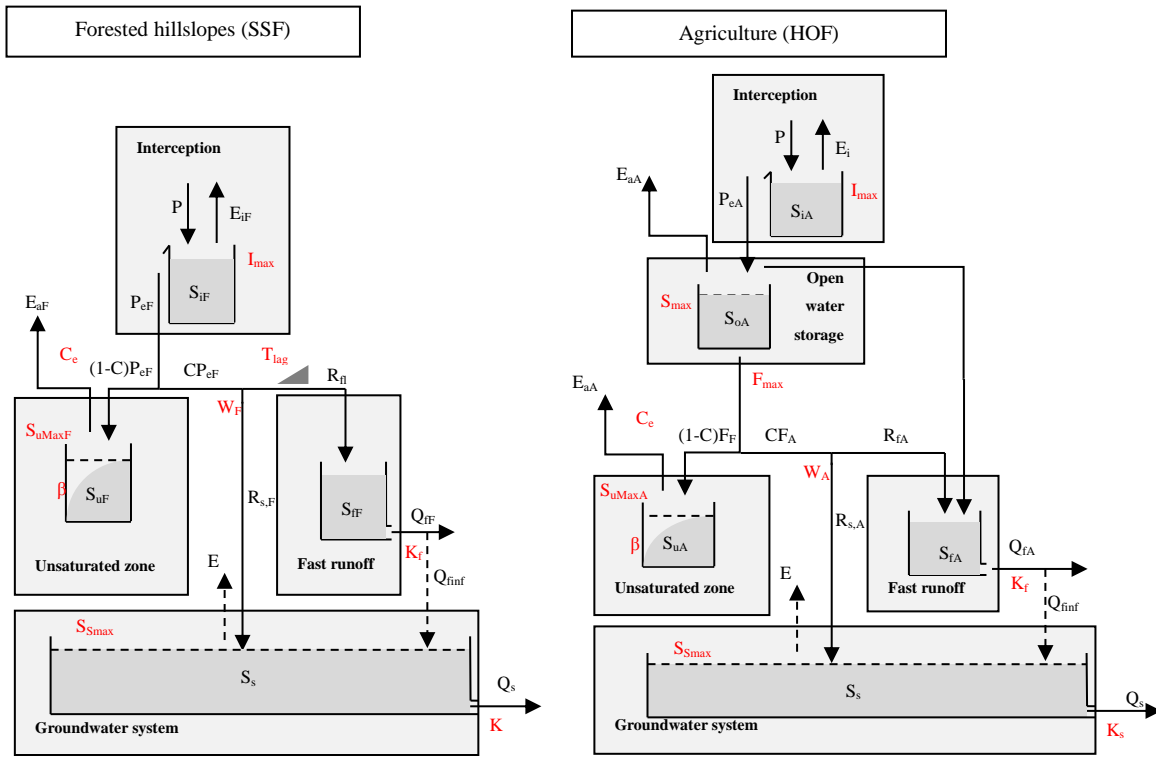
205

Figure 6: Model structure of the HRUs: *Forested hillslopes* **(left) and** *Agriculture* **(right). The structure for** *Shrubs on hillslopes* **is similar to the left one replacing the indices F with S. The structure for** *Grassland* **is similar to the right one replacing the indices A with G. Parameters are marked in red, storages and fluxed in black. Symbol explanation:** Fluxes**: precipitation (*P*), evaporation of the interception zone (*E_i*), actual evaporation (*E_a*), evaporation from groundwater only applied in the sub-catchment Sand (*E_s*),**

210 **effective precipitation (*P_e*), infiltration into the unsaturated zone (*F_A*), discharge from unsaturated zone to the fast runoff zone (*R_f*), groundwater recharge (*R_s*), discharge from the fast runoff (*Q_f*), infiltration into groundwater system only applied in the sub-catchment Sand (*Q_{f, inf}*), discharge from the slow runoff (*Q_s*).** Storages**: storage in the interception zone (*S_i*), open water storage (*S_{oA}*), storage in the root zone (*S_u*), storage for the slow runoff (*S_s*), storage for the fast runoff (*S_f*).** Remaining symbols**: splitter (*W*), splitter (*C*), soil moisture distribution coefficient (*β*), transpiration coefficient (*C_e* = 0.5), reservoir coefficient (*K*); indices f and s**

215 **indicate the fast and slow runoff.** Units**: fluxes [mm/d], storages [mm], reservoir coefficient [d], remaining parameters [-].**

3.3 Model constraints

Parameters and process constraints were applied to eliminate unrealistic parameter combinations and constrain the flow volume. Parameter constraints were applied to the maximum interception, reservoir coefficients, the storage capacity in the root zone or on the surface, and the slope-roughness parameter, Table 5. Process constraints were applied to the runoff

220 coefficient, groundwater recharge, interception and infiltration, Table 6. The effect of including these parameter and process constraints is illustrated in Figure S5. For instance, the maximum storage in the unsaturated zone $S_{u,max}$ equals the root zone storage capacity and was estimated using the method of Gao (2014) based on remotely sensed precipitation and evaporation (Gao et al., 2014b;Wang-Erlandsson et al., 2016). The dry season evaporation has been derived from the actual evaporation using the NDVI.

225

Table 5: Overview of all parameter constraints applied in the hydrological model for the Mara River Basin

Parameter	Symbol	Formula	Comment
Interception	I_{max}	$I_{max,forest} > I_{max,grass}, I_{max,shrubs}, I_{max,cropland}$ $I_{max,shrubs} > I_{max,grass}, I_{max,cropland}$	Based on perception
Reservoir coefficient	K_s, K_f	$K_s > K_f$	Based on perception
Storage capacity in unsaturated zone	$S_{u, max}$	$S_{R,y_i} = \int P_e - E_d \, dt$ With: $\dfrac{E_d}{E_a} = \dfrac{\text{NDVI}_D}{\text{NDVI}_A}$ thus: $E_d = E_a * \dfrac{\text{NDVI}_D}{\text{NDVI}_A}$	Based on NDVI, equivalent to the root zone storage capacity (Gao et al., 2014b) $S_{R, yi}$: required storage for year i P_e: effective rainfall over dry season E_d: annual mean dry season evaporation, calculated assuming a linear relation between the evaporation and the NDVI E_a: actual mean annual evaporation NDVI_D: annual mean dry season NDVI NDVI_A: annual mean actual NDVI Through a statistical analysis of S_R using the Gumbel distribution, the storage capacity $S_{u, max}$ with a return period of 20 years is calculated.
Reservoir coefficient for groundwater system	K_s	$Q_s = Q_{t=0} * exp\left(-\dfrac{t}{K_s}\right)$	Based on hydrograph recession analysis Q_s: groundwater discharge
Maximum surface water storage	S_{max}	-	Based on DEM assuming S_{max} is equal to the sink volumes
Slope-roughness parameter	c	$Q = c * A * R^{\frac{2}{3}} = u * A$ $u = c * R^{\frac{2}{3}} \rightarrow c_{calculated} = \dfrac{u}{R^{\frac{2}{3}}}$ $c_{calculated,-25\% \, error} < c < c_{calculated,+25\% \, error}$	Based on Strickler formula, cross-section data and a single discharge and velocity measurement at Mines allowing a wide error margin of 25%

Table 6: Overview of all process constraints applied in the hydrological model for the Mara River Basin

Process	Symbol	Formula	Comment
Average annual runoff coefficient	C	$C = 1 - \dfrac{E}{P} = e^{-\frac{E_p}{P}}$	Based on the Budyko curve using the 95% percentile, hence the modelled average annual runoff coefficient should be below the 95-percentile of the observations
Groundwater recharge	R_s	$R_{s,F} > R_{s,C}, R_{s,G}$	Based on the assumption that deeper rooting vegetation creates preferential drainage patterns
Annual interception	E_i	$E_{i,F} > E_{i,G}, E_{i,S}$	Based on the assumption that the interception is higher in forests than in grassland and shrublands
Fast runoff infiltration	-	$f_{Q_{river}} < 3 \, \mathrm{yr}^{-1}$	Frequency of river runoff. Based on interviews, locals seldom observed runoff more than 3 times a year.

230

3.4 Model calibration method using water levels

The hydrological model was calibrated on a daily timescale applying the MOSCEM-UA algorithm (Vrugt et al., 2003) with parameter ranges and values as indicated in Table S1 and S2. For the calibration, the Nash-Sutcliffe coefficient (Nash and Sutcliffe, 1970) was applied to the water level duration curve (Eq.1 linear, and Eq.2 log-scale). This frequently used

235 objective function is advantageous as it is sensitive to high flows, but also to low flows when using logarithmic values (Krause et al., 2005;McCuen Richard et al., 2006;Pushpalatha et al., 2012). By calibrating on the duration curve, the focus is on the flow statistics and not on the timing of individual flow peaks. This information is also in the time series. This is justified since there were high uncertainties in the timings of floods events due to the limited number of available rainfall stations to capture the spatial variability of the rainfall input well. Therefore, duration curves were considered as a good

240 signature for calibrating this model; this was also concluded in previous studies (Westerberg et al., 2011;Yadav et al., 2007).

$$\mathrm{NS_d} \quad = 1 - \frac{\Sigma\left(h_{mod,sorted} - h_{obs,sorted}\right)^2}{\Sigma\left(h_{obs,sorted} - h_{obs,avg}\right)^2} \tag{1}$$

$$\mathrm{NS_{log(d)}} = 1 - \frac{\Sigma\left(\log\left(h_{mod,sorted}\right) - \log\left(h_{obs,sorted}\right)\right)^2}{\Sigma\left(\log\left(h_{obs,sorted}\right) - \log\left(h_{obs,avg}\right)\right)^2} \tag{2}$$

For the water level based calibration, the modelled discharge needs to be converted to modelled water level. This calculation was done with the Strickler-Manning formula in which the discharge is a function of the water level (Eq. (3)), where R is the hydraulic radius (Eq. (6)), A the cross-sectional area (Eq. (5)), i the slope, k the roughness and c the slope-roughness

parameter (Eq. (4)). The hydraulic radius and cross-section are a function of the water depth d which is the water level

245 subtracted h by the reference level h_0 (Eq. (7)). The cross-sections were simplified as a trapezium with river width B and two different river bank slopes i_1 and i_2; these coefficients (Table 7) were estimated based on the available cross-section information (Figures S6 – S8). Since the slope and roughness are unknown, the slope-roughness parameter c was calibrated.

$$Q = k * i^{\frac{1}{2}} * A * R^{\frac{2}{3}} = c * A * R^{\frac{2}{3}} \tag{3}$$

$$c = k * i^{\frac{1}{2}} \tag{4}$$

$$A = B * d + \frac{1}{2} * d * (i_1 + i_2) * d \tag{5}$$

$$R = \frac{A}{B + d * \left((1 + i_1^2)^{\frac{1}{2}} + (1 + i_2^2)^{\frac{1}{2}} \right)} \tag{6}$$

$$d = h - h_0 \tag{7}$$

Table 7: Coefficients used for the river cross-section

	River width B [m]	River bank slope i_1 [-]	River bank slope i_2 [-]	Reference level h_0 [m]
Amala	10.0	3.50	1.83	0
Nyangores	19.05	2.65	5.56	0
Mines	43.81	3.53	3.66	10

250

This model calibration method, illustrated graphically in Figure 7, was applied to three basins individually: the entire river basin using the station Mines, and for the sub-catchments Nyangores and Amala. At each location, the model was calibrated and validated for time periods indicated in Table 8; at Mines two time periods were used for validation to maximise the use

255 of the available ground measurements.

Table 8: Time periods used for the calibration and validation at three basins: Mines, Nyangores and Amala

	Mines	Nyangores	Amala
Calibration time period	1970-1974	1970-1980	1991-1992
Validation time period	1980-1981	1981-1992	1985-1986
	1982-1983		
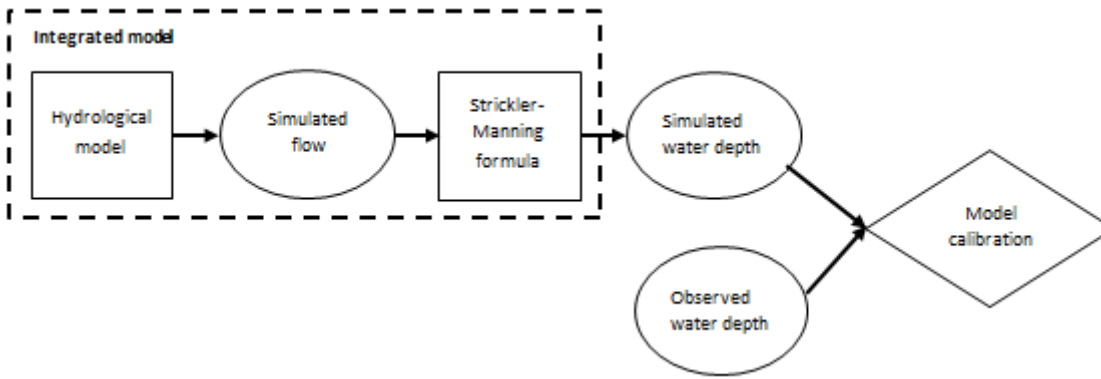
260

Figure 7: Flow chart of the proposed calibration method

3.5 Rating curve analysis

After calibration, the modelled water levels and discharges were analysed. For the model calibration and validation, the modelled and recorded water levels were compared at basin level, focusing on the time series and the duration curves.

265   Hereafter, water level – discharge relations were analysed taking two rating curves into consideration:

- "Recorded rating curve", relating Q_{rec} to h_{obs},
- "Geometric rating curve", relating $Q_{Strickler}$ to h_{obs}.

The geometric rating curve relates the modelled discharge $Q_{Strickler}$ to the observed water level h_{obs}. This discharge $Q_{Strickler}$ was calculated with the Strickler-Manning formula using the calibrated slope-roughness parameter c, cross-section data, and

270   the observed water level $h_{obs.}$ Therefore, the equation behind the geometric rating curve basically is the Strickler-Manning formula (Eq. (3)) instead of the traditional rating curve equation (Eq. (8)). The advantage of the Strickler-Manning formula is that only one parameter is unknown (river bed slope and roughness c, Eq. (4)), instead of two (fitting parameters a, and b). However, the Strickler-Manning rating curve approach requires additional information on the cross-section.

$$Q = a * (h - h_0)^b \tag{8}$$

275

4 Results and discussion

4.1 Water level time series and duration curve

Model results were analysed graphically (Figure 8 to Figure 10 and Figure S9 to Figure S19) and numerically based on the
280 Nash-Sutcliffe values for the objective functions (Table 9). The results of the objective functions indicate that at Nyangores and Mines the calibration and validation results were consistent. At Mines, the modelled water level was simulated well, particularly with regard to the duration curve (Figure 8). At individual events, there were substantial differences. In some years, for example in 1974, the observed data were very well represented by the model outcome, however, in other years this was not the case. In general, the model captured the dynamics in the water level well. This was the case during both
285 calibration and validation (see Figure S12 and S13).

At Nyangores the observed and modelled water levels were also similar during calibration and validation, extreme high flows excluded (Figure 9). However, at Amala, the observed and modelled water levels differed significantly during calibration (Figure 10) and validation (Figure S15). The model missed several discharge events completely, likely related to missing rain fall events in the input data due to the high heterogeneity in precipitation.

290

Table 9: Overview of the values of the objective functions for each model simulation. Calibration was done based on the water level: $NS_{log(h)}$ and NS_h; for comparison, objective functions using the discharge were added here as well

	Nyangores		Amala		Mines		
	Calibration	Validation	Calibration	Validation	Calibration	Validation 1	Validation 2
$NS_{log(d)}$	0.92	0.75	0.92	-0.23	0.97	0.81	0.93
NS_d	0.80	0.69	0.26	0.37	0.97	0.92	0.89
$NS_{log(Q)}$	0.92	0.69	0.57	0.63	0.97	0.81	0.93
NS_Q	0.55	0.37	0.08	-1.67	0.90	0.76	0.77
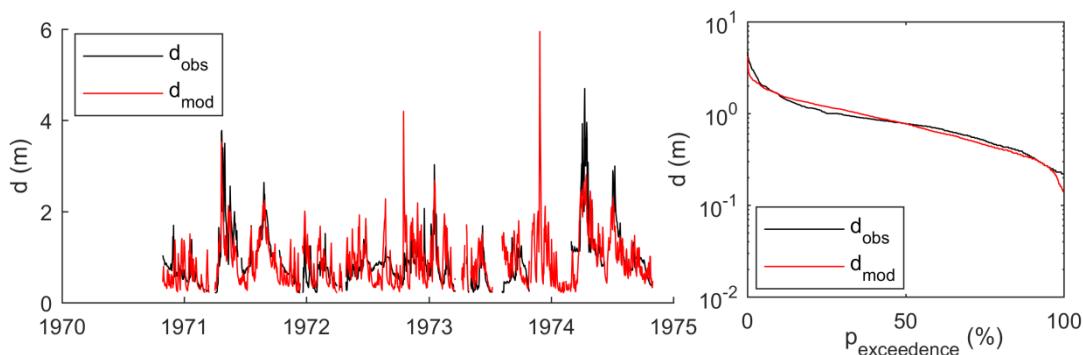
295

Figure 8: Model results at Mines during calibration: water depth time series and water depth exceedance
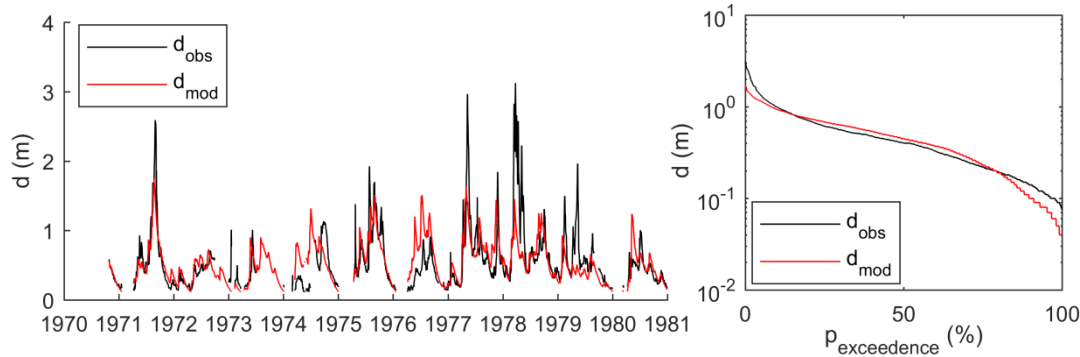
Figure 9: Model results at Nyangores during calibration: water depth time series and water depth exceedance
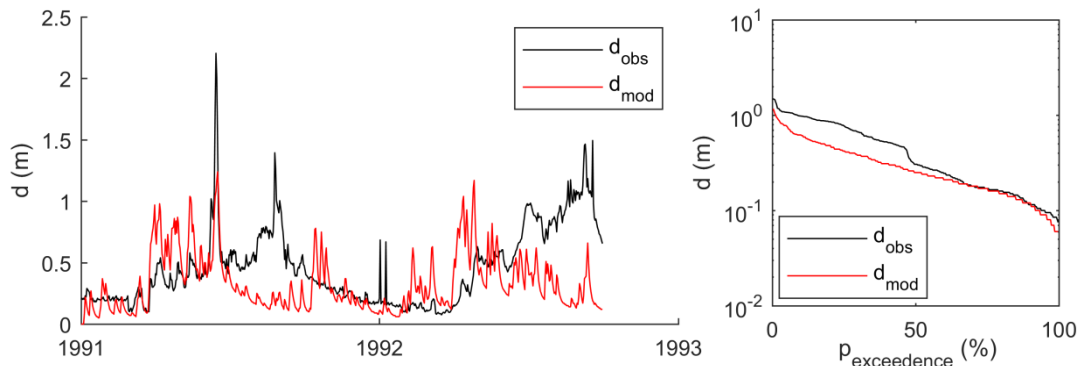
300 **Figure 10: Model results at Amala during calibration: water depth time series and water depth exceedance**

4.2 Discharge at sub-catchment level

At Mines, the discharge originates from seven different sub-catchments, each with a different contribution. Based on field observations, the mountainous upstream sub-catchments from the north should have the largest contribution whereas the contribution from the relatively drier and flatter Lemek and Talek tributaries from the eastern part of the catchment should
305 be relatively low. The contribution of each sub-catchment to the total modelled discharge was assessed on a monthly timescale and compared with observations.

As shown in Figure 11, the contribution varied throughout the year. In the summer (July-September), the modelled discharge mainly originates from the northern sub-catchments, Nyangores and Amala. However, in the winter (November-April), the modelled discharge mainly originates from the Sand and Lower sub-catchments. The eastern Middle, Talek and Lemek sub-
310 catchments have the lowest discharge throughout the entire year just as observed.
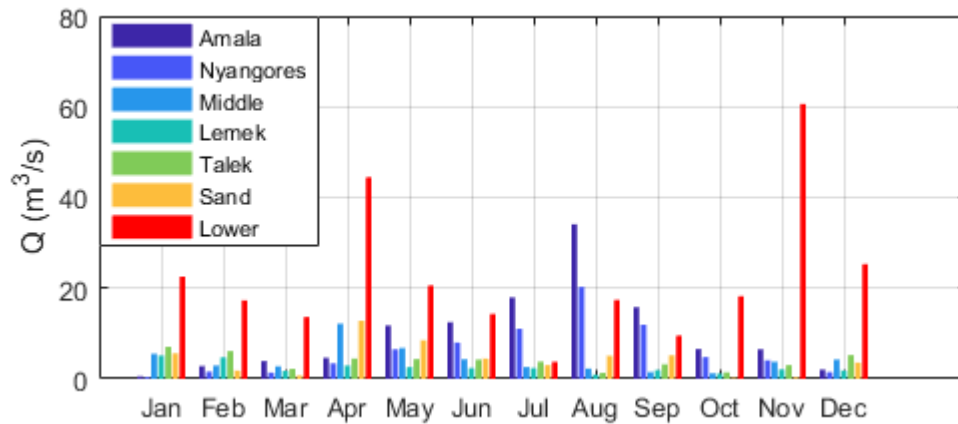
Figure 11: Monthly averaged modelled discharge for each sub-catchment

In previous studies, it has been shown that only a few discharge measurements can contain sufficient information to constrain model predictive uncertainties effectively (Seibert and Beven, 2009). To evaluate the model at sub-catchment

315 level, model results were compared with discharge measurements done during field trips in September/October 2014 at Emarti Bridge, Serena Pump House and New Mara Bridge. At all three locations, the point measurements fitted well within the range of the modelled discharge (see Figure 12).
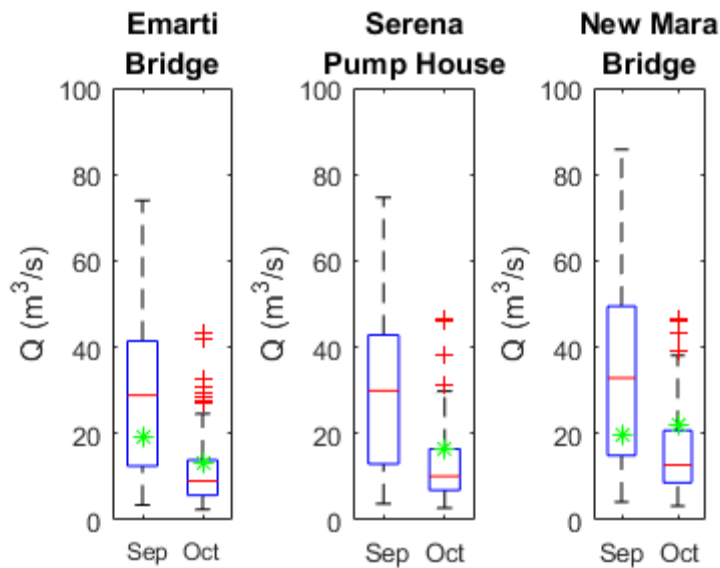
Figure 12: Boxplot of the modelled discharge at three locations; the green asterix represents the measured discharge in Sep/Oct
320 **2014**

4.3 Rating curve analysis

In this study, the recorded and geometric (Strickler-Manning) rating curves were compared (Figure 13). At Mines, these two rating curves differed significantly. For medium to high flows, both rating curves, recorded and geometric, run parallel indicating similar cross-sectional properties; only the off-set differed through changing river bed levels. On the other hand, the simulated cross-section average flow velocity were realistic compared to the point measurements at Mines indicating that velocities are greater than 2 m/s during high flows (see Figure 13). At Nyangores, the recorded and geometric rating curves were almost identical, while there were significant differences at Amala gauging station, especially in the low flows. Interestingly, these observations also hold for the validation period for all three stations.

The difference between the recorded and geometric rating curves at Mines probably resulted from uncertainties in the available recorded discharge data. In the complete discharge – water level graphs for all available data (Figure S2), large scatter was found. This could be the result of natural variability in the reference water level h_0 in the rating curve equation which was not taken into account. A sensitivity analysis of the recorded rating curve equation at Mines showed that a deviation of 0.1 m in the reference water level could alter the discharge with 4% for high flows and 46% for low flows. However, a deviation of 0.5 m resulted in a 19% – 325% change in the discharge. Therefore, unnoticed variations in the river bed level strongly affects the uncertainty in the recorded rating curve at Mara Mines, which is located in a morphologically dynamic section of the river (Stoop, 2017).

At Amala, the difference between both rating curves could be related to the effect of missing rain events in the input data as result of the short time series for calibration and validation. This resulted in absent discharge peaks and hence an underestimation of the flow; most extremely at Amala. During model calibration, this was compensated by increasing the parameter c in the Strickler-Manning formula (Eq. (4)). As a result, discharge values during missed events were increased, but also for all other days. The compensation effect was limited though since the model was calibrated on the duration curves instead of the time series. As parameter c is linearly related to the geometric rating curve (Eq. (3)), the latter was overestimated as well. Therefore, missing rain events in the input data resulted in the overestimation of the geometric rating curve.

In short, at the two stations with inconsistent rating curves, Amala and Mines, the geometric rating curve deviated significantly from the recordings. Strikingly, the deviations were observed at the same flow magnitudes where large inconsistencies were found in the observations, for instance in the low flows at Amala. However, at the gauging station with a reliable rating curve, Nyangores, the geometric and recorded discharge-water level relations were almost identical.
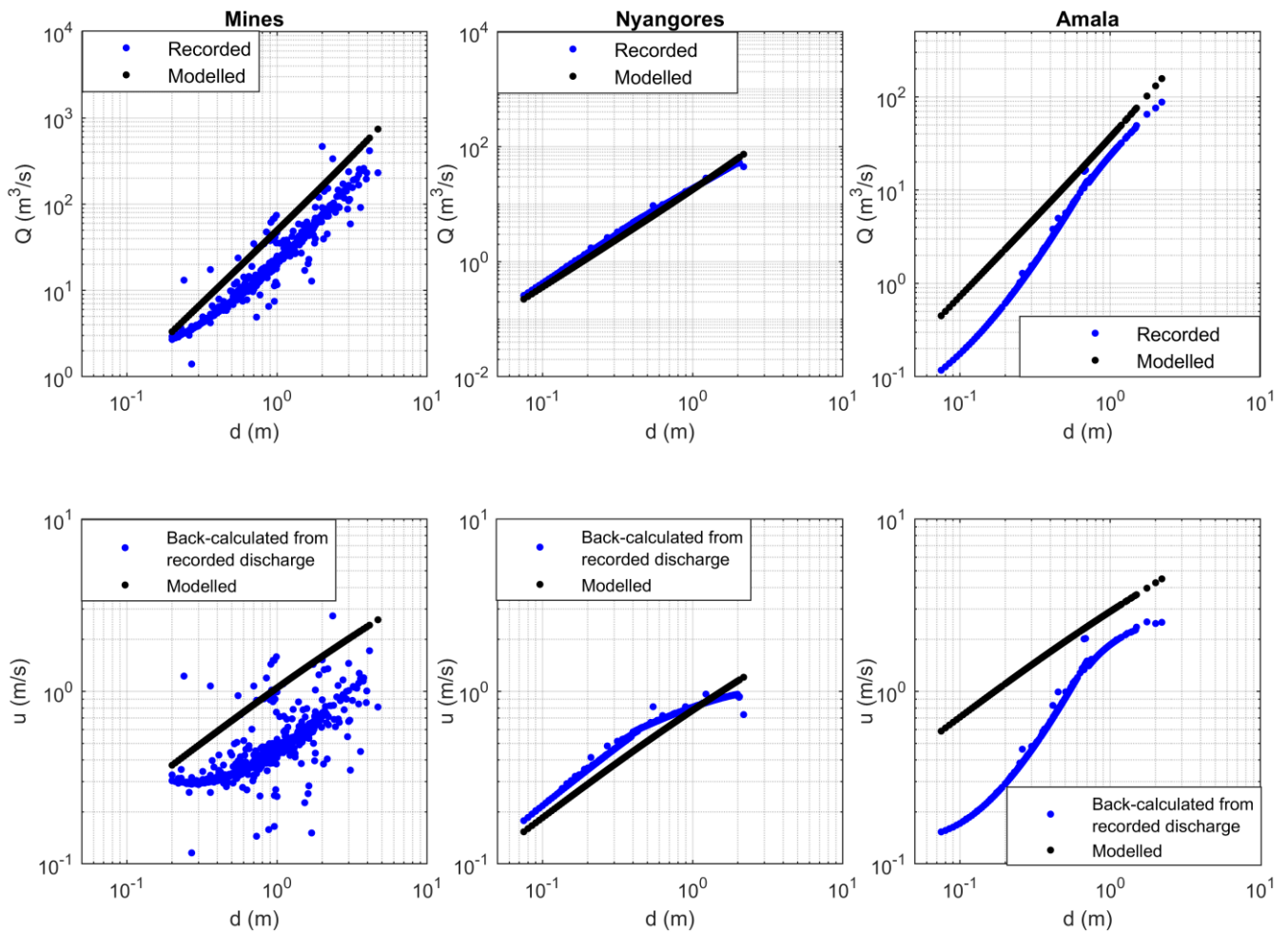
350

Figure 13: Model calibration results at Mines, Nyangores and Amala: Discharge – water depth graphs (upper) and velocity – water depth graphs (lower).

4.5 Limitations

355 This paper illustrated that the proposed water level calibration method simulated the discharge-water level relation well for the gauging station where consistent rating curve information was available. However, there are several limitations to this method. First, the slope-roughness parameter compensates for non-closure effects in the water balance, for instance due to errors in the precipitation which is extremely heterogeneous in semi-arid Mara basin. Unfortunately, this heterogeneity is poorly described in our study area with the available rain gauges (see section S7.2 on the precipitation data analysis)

360 influencing the modelling results. Therefore, this parameter should be constrained to minimize this compensation as much as possible. Second, the cross-section was assumed to be constant during the modelling time period. Data analyses indicated that expected changes in the river width or slope cannot affect the rating curve significantly. However, if this is not the case, then this cross-section change should be included during the model calibration.

. In previous studies, river water level time series were used for model calibration by using the Spearman rank correlation

365 function (Seibert and Vis, 2016) or an inverse rating curve to convert the modelled discharge to water level (Jian et al., 2017). Compared to these approaches, the calibration method proposed in this paper has the following advantages: 1) water level time series are direct measurements and therefore more reliable compared to processed data such as satellite based measurements, 2) merely one new calibration parameter (the slope-roughness parameter) is introduced instead of three when using an inverse rating curve, and 3) the model is calibrated on water level magnitudes instead of only the ranks which

370 would introduce biases. However, this method also has several disadvantages: 1) cross-section information is needed and is assumed to be constant over the time period for which it is applied, and 2) the newly introduced slope-roughness parameter compensates for non-closure effects in the water balance when not constrained well.

5 Summary and Conclusion

The goal of this paper was to illustrate a new calibration method using water level time series and the Strickler-Manning

375 formula instead of discharge in a semi-arid and poorly gauged basin. This method offers a potential alternative for calibration on discharge data, as is common practice also in poorly gauged catchments. The semi-distributed rainfall-runoff modelling framework FLEX-Topo was applied. The catchment was divided into four hydrological response units (HRUs) and seven sub-catchments based on the river tributaries. For each HRU, a unique model structure was defined based on the observed dominant flow processes. By constraining the parameters and processes, unrealistic parameter sets were excluded

380 from the calibration parameter set and the flow volume was constrained. This model was calibrated based on water levels to capture the flow dynamics. For this purpose, the modelled discharge was converted to water levels using the Strickler-Manning formula. The unknown slope-roughness parameter was calibrated.

An important output of this calibration approach is the "geometric rating curve equation" which relates the discharge to the water level using the Strickler-Manning formula. The geometric and recorded rating curves were significantly different at the

385 following two gauging stations: Mines, the catchment outlet, and Amala, a sub-catchment outlet. At both locations, the deviations were at the same flow magnitudes where large inconsistencies were found in the observations. However, at the gauging station with a reliable rating curve, Nyangores, the recorded and geometric discharge-water level relations were almost identical. In conclusion, this calibration method allows reliable simulations of the discharge-water level relation, even in a data poor region.

390 In addition, this paper analysed the current status of the hydro-meteorological network in the Mara River Basin focusing on the data availability and quality. Moreover, a hydrological model and an improved geometric rating curve equation were developed for this river. All three aspects contribute to improving the assessment of the water resources availability in the Mara River Basin.

For future studies, it would be interesting to apply this calibration method to other study river basins with different climatic

395 conditions and better data availability. Furthermore, it is recommended to assess the effect of rainfall uncertainties on this

calibration method. Moreover, the hydrological model was calibrated on two signatures and two objective functions only. However, it has not been analysed whether these signatures and objective functions provide sufficient information for calibration. Therefore, the procedures for water level based calibration should be analysed in more detail.

Acknowledgement

400 This research was part of the MaMaSe project (Mau Mara Serengeti) led by IHE Delft. Station data (discharge, water level and precipitation) was provided by the Water Resource Management Authority (WRMA) in Kenya. Temperature and additional precipitation data was obtained from NOAA online database (Menne et al., 2012).

References

Alvisi, S., Mascellani, G., Franchini, M., and Bárdossy, A.: Water level forecasting through fuzzy logic and artificial neural
405 network approaches, Hydrology and Earth System Sciences Discussions, 10, 1-17, 2006.
Beven, K. J.: Rainfall-runoff modelling : the primer, 2012.
Bulygina, N., and Gupta, H.: Correcting the mathematical structure of a hydrological model via Bayesian data assimilation, Water Resources Research, 47, n/a-n/a, 10.1029/2010WR009614, 2011.
Clarke, R. T.: Uncertainty in the estimation of mean annual flood due to rating-curve indefinition, Journal of Hydrology,
410 222, 185-190, 10.1016/S0022-1694(99)00097-9, 1999.
Dessu, S. B., Melesse, A. M., Bhat, M. G., and McClain, M. E.: Assessment of water resources availability and demand in the Mara River Basin, CATENA, 115, 104-114, http://dx.doi.org/10.1016/j.catena.2013.11.017, 2014.
Di Baldassarre, G., and Montanari, A.: Uncertainty in river discharge observations: a quantitative analysis, Hydrol. Earth Syst. Sci., 13, 913-921, 10.5194/hess-13-913-2009, 2009.
415 Di Baldassarre, G., and Claps, P.: A hydraulic study on the applicability of flood rating curves, Hydrology Research, 42, 10-19, 10.2166/nh.2010.098, 2011.
Di Baldassarre, G., Laio, F., and Montanari, A.: Effect of observation errors on the uncertainty of design floods, Physics and Chemistry of the Earth, Parts A/B/C, 42–44, 85-90, http://dx.doi.org/10.1016/j.pce.2011.05.001, 2012.
Domeneghetti, A., Castellarin, A., and Brath, A.: Assessing rating-curve uncertainty and its effects on hydraulic model
420 calibration, Hydrology and Earth System Sciences, 16, 1191-1202, 10.5194/hess-16-1191-2012, 2012.
Gao, H., Hrachowitz, M., Fenicia, F., Gharari, S., and Savenije, H. H. G.: Testing the realism of a topography-driven model (FLEX-Topo) in the nested catchments of the Upper Heihe, China, Hydrol. Earth Syst. Sci., 18, 1895-1915, 10.5194/hess-18-1895-2014, 2014a.
Gao, H., Hrachowitz, M., Schymanski, S. J., Fenicia, F., Sriwongsitanon, N., and Savenije, H. H. G.: Climate controls how
425 ecosystems size the root zone storage capacity at catchment scale, Geophysical Research Letters, 41, 2014GL061668, 10.1002/2014GL061668, 2014b.
Getirana, A. C. V.: Integrating spatial altimetry data into the automatic calibration of hydrological models, Journal of Hydrology, 387, 244-255, http://dx.doi.org/10.1016/j.jhydrol.2010.04.013, 2010.
Gharari, S., Hrachowitz, M., Fenicia, F., Gao, H., and Savenije, H. H. G.: Using expert knowledge to increase realism in
430 environmental system models can dramatically reduce the need for calibration, Hydrol. Earth Syst. Sci., 18, 4839-4859, 10.5194/hess-18-4839-2014, 2014.
GLOWS-FIU: Environmental Flow Recommendation for the Mara River, Kenya and Tanzania, in, Global Water for Sustainability program (GLOWS). Miami, FL, 2012.
Guerrero, J. L., Westerberg, I. K., Halldin, S., Xu, C. Y., and Lundin, L. C.: Temporal variability in stage-discharge
435 relationships, Journal of Hydrology, 446-447, 90-102, 10.1016/j.jhydrol.2012.04.031, 2012.

Hrachowitz, M., Savenije, H. H. G., Blöschl, G., McDonnell, J. J., Sivapalan, M., Pomeroy, J. W., Arheimer, B., Blume, T., Clark, M. P., Ehret, U., Fenicia, F., Freer, J. E., Gelfan, A., Gupta, H. V., Hughes, D. A., Hut, R. W., Montanari, A., Pande, S., Tetzlaff, D., Troch, P. A., Uhlenbrook, S., Wagener, T., Winsemius, H. C., Woods, R. A., Zehe, E., and Cudennec, C.: A decade of Predictions in Ungauged Basins (PUB)—a review, Hydrological Sciences Journal, 58, 1198-1255,

440   10.1080/02626667.2013.803183, 2013.

Jalbert, J., Mathevet, T., and Favre, A. C.: Temporal uncertainty estimation of discharges from rating curves using a variographic analysis, Journal of Hydrology, 397, 83-92, 10.1016/j.jhydrol.2010.11.031, 2011.

Jian, J., Ryu, D., Costelloe, J. F., and Su, C.-H.: Towards hydrological model calibration using river level measurements, Journal of Hydrology: Regional Studies, 10, 95-109, https://doi.org/10.1016/j.ejrh.2016.12.085, 2017.

445   Karamuz, E., Osuch, M., and Romanowicz, R. J.: The influence of rating curve uncertainty on flow conditions in the River Vistula in Warsaw, in: GeoPlanet: Earth and Planetary Sciences, 153-166, 2016.

Krause, P., Boyle, D. P., and Bäse, F.: Comparison of different efficiency criteria for hydrological model assessment, Advances in Geosciences, 5, 89-97, 10.5194/adgeo-5-89-2005, 2005.

Kuczera, G.: Correlated rating curve error in flood frequency inference, Water Resources Research, 32, 2119-2127,

450   10.1029/96WR00804, 1996.

Liu, W.-C., and Chung, C.-E.: Enhancing the Predicting Accuracy of the Water Stage Using a Physical-Based Model and an Artificial Neural Network-Genetic Algorithm in a River System, Water, 6, 10.3390/w6061642, 2014.

Mati, B. M., Mutie, S., Gadain, H., Home, P., and Mtalo, F.: Impacts of land-use/cover changes on the hydrology of the transboundary Mara River, Kenya/Tanzania, Lakes & Reservoirs: Research and Management, 13, 169-177, 2008.

455   McClain, M. E., Subalusky, A. L., Anderson, E. P., Dessu, S. B., Melesse, A. M., Ndomba, P. M., Mtamba, J. O. D., Tamatamah, R. A., and Mligo, C.: Comparing flow regime, channel hydraulics and biological communities to infer flow-ecology relationships in the Mara River of Kenya and Tanzania, Hydrological Sciences Journal, 59 (3-4), 1-19, 10.1080/02626667.2013.853121, 2013.

McCuen Richard, H., Knight, Z., and Cutter, A. G.: Evaluation of the Nash–Sutcliffe Efficiency Index, Journal of

460   Hydrologic Engineering, 11, 597-602, 10.1061/(ASCE)1084-0699(2006)11:6(597), 2006.

McMillan, H., Freer, J., Pappenberger, F., Krueger, T., and Clark, M.: Impacts of uncertain river flow data on rainfall-runoff model calibration and discharge predictions, Hydrological Processes, 24, 1270-1284, 10.1002/hyp.7587, 2010.

McMillan, H. K., and Westerberg, I. K.: Rating curve estimation under epistemic uncertainty, Hydrological Processes, 29, 1873-1882, 10.1002/hyp.10419, 2015.

465   Menne, M. J., Durre, I., Korzeniewski, B., McNeal, S., Thomas, K., Yin, X., Anthony, S., Ray, R., Vose, R. S., Gleason, B. E., and Houston, T. G.: Global Historical Climatology Network - Daily (GHCN-Daily), Version 3.12, http://doi.org/10.7289/V5D21VHZ, 2012.

Michailovsky, C. I., McEnnis, S., Berry, P. A. M., Smith, R., and Bauer-Gottwein, P.: River monitoring from satellite radar altimetry in the Zambezi River basin, Hydrol. Earth Syst. Sci., 16, 2181-2192, 10.5194/hess-16-2181-2012, 2012.

470   Morlot, T., Perret, C., Favre, A. C., and Jalbert, J.: Dynamic rating curve assessment for hydrometric stations and computation of the associated uncertainties: Quality and station management indicators, Journal of Hydrology, 517, 173-186, 10.1016/j.jhydrol.2014.05.007, 2014.

Nash, J. E., and Sutcliffe, J. V.: River flow forecasting through conceptual models part I — A discussion of principles, Journal of Hydrology, 10, 282-290, https://doi.org/10.1016/0022-1694(70)90255-6, 1970.

475   Paiva, R. C. D., Collischonn, W., Bonnet, M. P., de Gonçalves, L. G. G., Calmant, S., Getirana, A., and Santos da Silva, J.: Assimilating in situ and radar altimetry data into a large-scale hydrologic-hydrodynamic model for streamflow forecast in the Amazon, Hydrol. Earth Syst. Sci., 17, 2929-2946, 10.5194/hess-17-2929-2013, 2013.

Panda, R. K., Pramanik, N., and Bala, B.: Simulation of river stage using artificial neural network and MIKE 11 hydrodynamic model, Computers & Geosciences, 36, 735-745, https://doi.org/10.1016/j.cageo.2009.07.012, 2010.

480   Pelletier, P. M.: Uncertainties in the single determination of river discharge: a literature review, Canadian journal of civil engineering, 15, 834-850, 1988.

Pereira-Cardenal, S. J., Riegels, N. D., Berry, P. A. M., Smith, R. G., Yakovlev, A., Siegfried, T. U., and Bauer-Gottwein, P.: Real-time remote sensing driven river basin modeling using radar altimetry, Hydrol. Earth Syst. Sci., 15, 241-254, 10.5194/hess-15-241-2011, 2011.

485 Petersen-Øverleir, A.: Modelling stage-discharge relationships affected by hysteresis using the Jones formula and nonlinear regression, Hydrological Sciences Journal, 51, 365-388, 10.1623/hysj.51.3.365, 2006.

Pushpalatha, R., Perrin, C., Moine, N. L., and Andréassian, V.: A review of efficiency criteria suitable for evaluating low-flow simulations, Journal of Hydrology, 420-421, 171-182, https://doi.org/10.1016/j.jhydrol.2011.11.055, 2012.

Revilla-Romero, B., Beck, H. E., Burek, P., Salamon, P., de Roo, A., and Thielen, J.: Filling the gaps: Calibrating a rainfall-
490 runoff model using satellite-derived surface water extent, Remote Sensing of Environment, 171, 118-131, http://dx.doi.org/10.1016/j.rse.2015.10.022, 2015.

Rey, A., de Koning, D., Rongen, G., Merks, J., van der Meijs, R., and de Vries, S.: Water in the Mara Basin: Pioneer project for the MaMaSe project, Unpublished MSc project report, Delft University of Technology, 2015.

Ričko, M., Birkett, C. M., Carton, J. A., and Crétaux, J. F.: Intercomparison and validation of continental water level
495 products derived from satellite radar altimetry, Journal of Applied Remote Sensing, 6, 10.1117/1.JRS.6.061710, 2012.

Savenije, H. H. G.: Topography driven conceptual modelling (FLEX-Topo), Hydrol. Earth Syst. Sci., 14, 2681-2692, 2010.

Schwatke, C., Dettmering, D., Bosch, W., and Seitz, F.: DAHITI – an innovative approach for estimating water level time series over inland waters using multi-mission satellite altimetry, Hydrol. Earth Syst. Sci., 19, 4345-4364, 10.5194/hess-19-4345-2015, 2015.

500 Seibert, J., and Beven, K. J.: Gauging the ungauged basin: how many discharge measurements are needed?, Hydrol. Earth Syst. Sci., 13, 883-892, 10.5194/hess-13-883-2009, 2009.

Seibert, J., and Vis, M. J. P.: How informative are stream level observations in different geographic regions?, Hydrological Processes, 30, 2498-2508, 10.1002/hyp.10887, 2016.

Sellami, H., La Jeunesse, I., Benabdallah, S., and Vanclooster, M.: Parameter and rating curve uncertainty propagation
505 analysis of the SWAT model for two small Mediterranean catchments, Hydrological Sciences Journal, 58, 1635-1657, 10.1080/02626667.2013.837222, 2013.

Shahin, M.: Hydrology and Water Resources of Africa, Water Science and Technology Library, Springer Netherlands, 2002.

Sikorska, A. E., Scheidegger, A., Banasik, K., and Rieckermann, J.: Considering rating curve uncertainty in water level predictions, Hydrology and Earth System Sciences, 17, 4415-4427, 10.5194/hess-17-4415-2013, 2013.

510 Stoop, B. M.: Morphology of the Mara River: Assessment of the long term morphology and the effect on the riverine physical habitat, Delft University of Technology, 2017.

Sun, W., Ishidaira, H., and Bastola, S.: Calibration of hydrological models in ungauged basins based on satellite radar altimetry observations of river water level, Hydrological Processes, 26, 3524-3537, 10.1002/hyp.8429, 2012.

Sun, W., Ishidaira, H., Bastola, S., and Yu, J.: Estimating daily time series of streamflow using hydrological model
515 calibrated based on satellite observations of river water surface width: Toward real world applications, Environmental Research, 139, 36-45, http://dx.doi.org/10.1016/j.envres.2015.01.002, 2015.

Thyer, M., Renard, B., Kavetski, D., Kuczera, G., and Clark, M.: Improving hydrological model predictions by incorporating rating curve uncertainty, in, Engineers Australia, Australia, Proceedings of the 34th IAHR World Congress, 2011: pp.1546-1553, 2011.

520 Tomkins, K. M.: Uncertainty in streamflow rating curves: Methods, controls and consequences, Hydrological Processes, 28, 464-481, 10.1002/hyp.9567, 2014.

Tourian, M. J., Schwatke, C., and Sneeuw, N.: River discharge estimation at daily resolution from satellite altimetry over an entire river basin, Journal of Hydrology, 546, 230-247, https://doi.org/10.1016/j.jhydrol.2017.01.009, 2017.

Digital Elevation Map: www.earthexplorer.usgs.gov, 2014.

525 van Meerveld, H. J. I., Vis, M. J. P., and Seibert, J.: Information content of stream level class data for hydrological model calibration, Hydrol. Earth Syst. Sci., 21, 4895-4905, 10.5194/hess-21-4895-2017, 2017.

Vrugt, J. A., Gupta, H. V., Bastidas, L. A., Bouten, W., and Sorooshian, S.: Effective and efficient algorithm for multiobjective optimization of hydrologic models, Water Resources Research, 39, n/a-n/a, 10.1029/2002WR001746, 2003.

Wang-Erlandsson, L., Bastiaanssen, W. G. M., Gao, H., Jägermeyr, J., Senay, G. B., van Dijk, A. I. J. M., Guerschman, J. P.,
530 Keys, P. W., Gordon, L. J., and Savenije, H. H. G.: Global root zone storage capacity from satellite-based evaporation, Hydrol. Earth Syst. Sci., 20, 1459-1481, 10.5194/hess-20-1459-2016, 2016.

Westerberg, I. K., Guerrero, J. L., Younger, P. M., Beven, K. J., Seibert, J., Halldin, S., Freer, J. E., and Xu, C. Y.: Calibration of hydrological models using flow-duration curves, Hydrol. Earth Syst. Sci., 15, 2205-2227, 10.5194/hess-15-2205-2011, 2011.

535   WMO: Guide to Hydrological Practices; Volume I Hydrology – From Measurement to Hydrological Information, 2008.

Yadav, M., Wagener, T., and Gupta, H.: Regionalization of constraints on expected watershed response behavior for improved predictions in ungauged basins, Advances in Water Resources, 30, 1756-1774, https://doi.org/10.1016/j.advwatres.2007.01.005, 2007.

Yan, K., Di Baldassarre, G., Solomatine, D. P., and Schumann, G. J. P.: A review of low-cost space-borne data for flood
540   modelling: topography, flood extent and water level, Hydrological Processes, 29, 3368-3387, 10.1002/hyp.10449, 2015.